J|A|C|S ARTICLES

Published on Web 02/19/2009

How the Substrate D-Glutamate Drives the Catalytic Action of *Bacillus subtilis* Glutamate Racemase

Eduard Puig,[†] Edgar Mixcoha,[†] Mireia Garcia-Viloca,[†,‡,*] Àngels González-Lafont,[†,‡] and José M. Lluch[†,‡]

Departament de Química and Institut de Biotecnologia i de Biomedicina, Universitat Autònoma de Barcelona, Bellaterra (Barcelona), Spain

Received July 31, 2008; E-mail: mireia@bioinf.uab.es

Abstract: Molecular Dynamics simulations with a Molecular Mechanics force field and a quite complete exploration of the QM/MM potential energy surfaces have been performed to study the D-glutamate → L-glutamate reaction catalyzed by *Bacillus subtilis* glutamate racemase. The results show that the whole process involves four successive proton transfers that occur in three different steps. The Michaelis complex is already prepared to make the first proton transfer (from Cys74 to Asp10) possible. The second step involves two proton transfers (from the α-carbon to Cys74, and from Cys185 to the α-carbon), which occurs in a concerted way, although highly asynchronic. Finally, in the third step, the nascent deprotonated Cys185 is protonated by His187. The positively charged ammonium group of the substrate plays a very important key role in the reaction. It accompanies each proton transfer in a concerted and coupled way, but moving itself in the opposite direction from Asp10 to His187. Thus, the catalytic action of *Bacillus subtilis* glutamate racemase is driven by its own substrate of the reaction, D-glutamate.

1. Introduction

D-Glutamate is an essential building block of the peptidoglycan layer of bacterial cell walls that protect the bacteria from osmotic lysis. Glutamate racemase (RacE, MurI, E.C. 5.1.1.3) is a pyridoxal-phosphate-independent enzyme that catalyzes the interconversion of L- and D-glutamate, so providing pathogenic bacteria with a source of D-glutamate. Thus, glutamate racemase has been considered a target for antibacterial drug design.[1−5]

The commonly accepted mechanism for catalysis by glutamate racemase involves deprotonation of the glutamate's α-proton, followed by substrate reprotonation on the opposite stereochemical face. Mutagenesis studies support the idea that two cysteines are the catalytic acid/base residues. These two cysteines are able to exchange their acid/base roles depending on which enantiomer binds the active site.[6−9] The two cysteines and some other residues close to the glutamate substrate are strictly conserved in all RacE and other cofactor-independent amino acid racemases, including aspartate racemase[10] and proline racemase.[11]

A very challenging problem behind that reaction is how glutamate racemase manages to catalyze fast proton exchange involving the α-carbon−hydrogen bond cleavage of glutamate, whose pK_a in aqueous solution is estimated to be higher than the value 21 of the fully protonated form of the amino acid because of the presence of the carboxylate anion.[8] This is confirmed by the carbon acidity of the glycine zwitterion (pK_a = 28.9 ± 0.5) calculated by Rios et al.[12] from their carbon deprotonation kinetic data. The situation is even more intriguing considering that a deprotonated cysteine should act as a general base catalyst. The pK_a of the cysteine side chain in aqueous solution is 8.4. So, the sulfur atom of the cysteine should be predicted to be almost fully protonated at neutral pH, being unable to receive the α-proton of the glutamate. However, it has been realized that the electrostatic field inside the enzyme (and, in particular, some specific interactions among residues) can highly perturb the original pK_a's in aqueous solution, making possible unlikely chemical processes.[13] A quite known example of that is the catalysis of the interconversion of L- and D-alanine by pyridoxal 5′-phosphate and alanine racemase, where Tyr265' and Lys39 are considered to be the two catalytic residues acting as an acid/base pair.[14−17] The pK_a's in aqueous solution of the

[†] Departament de Química.
[‡] Institut de Biotecnologia i de Biomedicina.

(1) Dios, de A.; Prieto, L.; Martin, J. A.; Rubio, A.; Ezquerra, J.; Tebbe, M.; deUralde, B. L.; Martin, J.; Sanchez, A.; LeTourneau, D. L.; McGee, J. E.; Boylan, C.; Parr, T. R.; Smith, M. C. *J. Med. Chem.* **2002**, *45*, 4559.
(2) Doublet, P.; van Heijenoort, J.; MenginLecreulx, D. *Microbial Drug Resistance-Mechanisms Epidemiology and Disease.* **1996**, *2*, 43.
(3) Schnell, B.; Faber, K.; Kroutil, W. *Adv. Synth. Catal.* **2003**, *345*, 653.
(4) Chu, D.; Plattner, J.; Katz, L. *Nat. Prod. Rep.* **1996**, *9*, 199.
(5) Fisher, S. L. *Microbial Biotechnol.* **2008**, *1*, 345.
(6) Glavas, S.; Tanner, M. E. *Biochemistry* **2001**, *40*, 6199.
(7) Glavas, S.; Tanner, M. E. *Biochemistry.* **1999**, *38*, 4106.
(8) Tanner, M. E. *Acc. Chem. Res.* **2002**, *35*, 237.
(9) Yoshimura, T.; Esaki, N. *J. Biosci. Bioeng.* **2003**, *96*, 103.
(10) Abe, K.; Takahashi, S.; Muroki, Y.; Kera, Y.; Yamada, R. H. *J. Biochem.* **2006**, *139*, 235.
(11) Buschiazzo, A.; Goytia, M.; Schaeffer, F.; Degrave, W.; Shepard, W.; Gregoire, C.; Chamond, N.; Cosson, A.; Berneman, A.; Coatnoan, N.; Alzari, P. M.; Minoprio, P. *Proc. Natl. Acad. Sci. U.S.A.* **2006**, *103*, 1705.
(12) Rios, A.; Amyes, T. L.; Richard, J. P. *J. Am. Chem. Soc.* **2000**, *122*, 9373.
(13) Schlippe, Y. V. G.; Hedstrom, L. *Arch. Biochem. Biophys.* **2005**, *433*, 266.
(14) Ondrechen, M. J.; Briggs, J. M.; McCammon, J. A. *J. Am. Chem. Soc.* **2001**, *123*, 2830.
(15) Sun, S.; Toney, M. D. *Biochemistry* **1999**, *38*, 4508.
(16) Major, D. T.; Nam, K.; Gao, J. *J. Am. Chem. Soc.* **2006**, *128*, 8114.
(17) Major, D. T.; Gao, J. *J. Am. Chem. Soc.* **2006**, *128*, 16345.

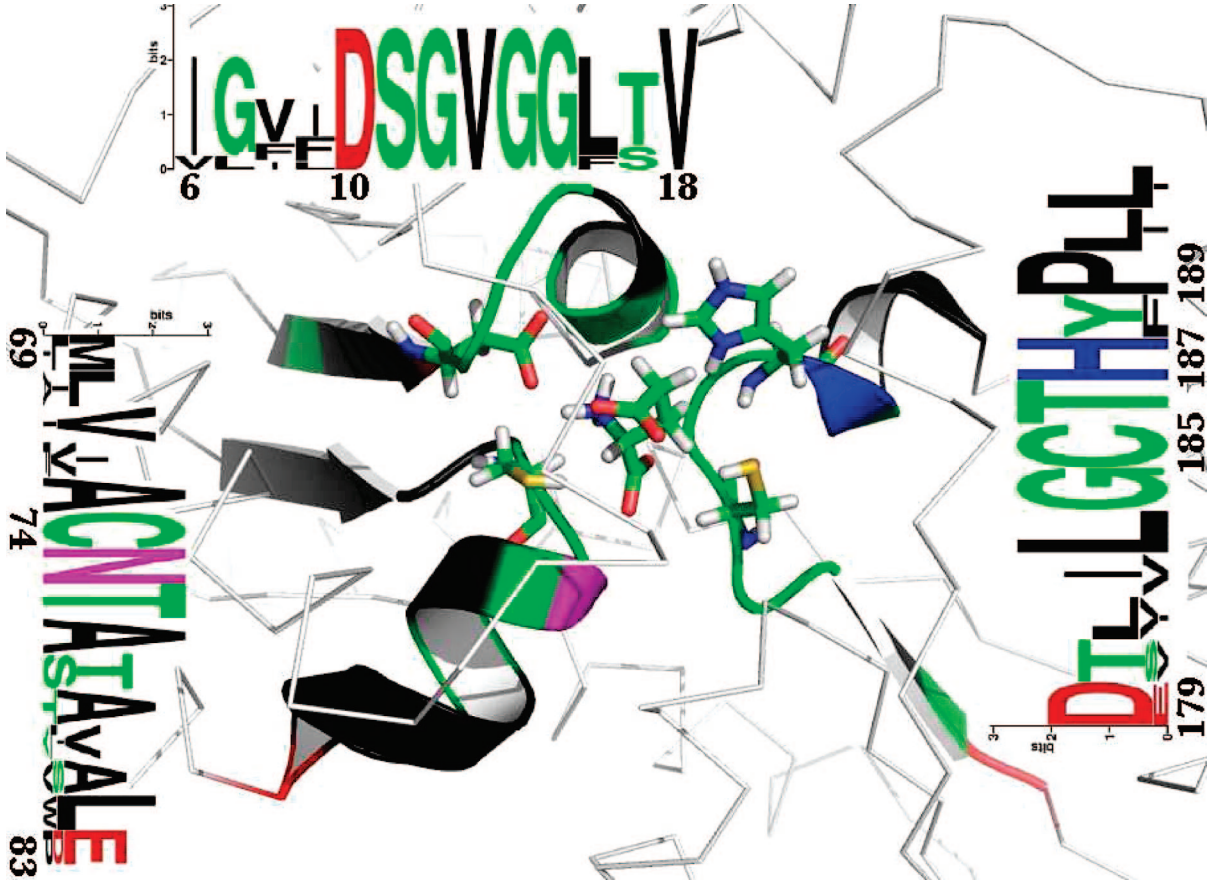

Figure 1. Glutamate racemases conserved motifs found in 8 different organisms. The figure shows the active site formation by three alpha-beta hairpins. Negatively charged residues colored in red, positively charged residues in blue, polar residues in violet, hidrophobic residues in black and non charged polar residues in green. The height of each letter indicates the degree of conservation of the residue among all the analyzed sequences.[22]

phenolic hydroxyl of tyrosine and the conjugate acid of lysine are both 10.5. So, both residues could be expected to be protonated at neutral pH. In spite of this, the electric field in the active site of alanine racemase stabilizes the formation of a negative charge in the phenolic oxygen atom of Tyr265′ (probably by the His166-mediated interaction with Arg219), so shifting the pK_a to 7.3[15] and allowing Tyr265′ to work as the catalytic base in the conversion of L-alanine to D-alanine at ∼pH = 8, where the enzyme is most likely active in nature.[14] In turn, the conjugate acid of Lys39 also has a shifted pK_a inside the active side, such that a significant fraction of Lys39 residues are unprotonated amines able to act as the catalytic base for the conversion of D-alanine to L-alanine.[14]

The structure of a complex of *Bacillus subtilis* RacE (BsRacE) with D-glutamate has been recently solved and refined to 1.75 Å resolution.[18] Analysis of this structure shows that the conserved thiol groups, Cys74 and Cys185, are close to the side chains of Asp10 (3.9 Å) and His187 (4.2 Å). Furthermore, the α-carbon of the D-glutamate substrate lies almost exactly on the line joining the two sulfurs at distances of only 3.5 and 4.4 Å to Cys74 and Cys185, respectively. Its α-amino is in close proximity to both cysteines, whereas its side chain carboxyl is close to only Cys74. In addition, there is a water-mediated contact between the side chain of the D-glutamate substrate and Glu153, which also simultaneously forms a hydrogen bond with His187, which, in turn, is adjacent to Cys185. All these relative positions of the residues in the active site of BsRacE support the mechanism proposed by Glavas and Tanner who suggested that both cysteines are neutral thiols most of the time.[19] The problem then is how the enzyme manages to deprotonate the catalytically active cysteines. Although on the basis of experimental studies for alanine racemase[20] or proline racemase[11] other possibilities could be imagined, mutagenesis studies[6] in the *Lactobacillus fermenti* glutamate racemase show that neighboring residues, Asp10 in the D → L direction and His186 (His187 in BsRacE) in the L → D direction, assist the catalytic thiols in acting as bases (the existence of a long life thiolate being no longer needed).

Analysis of the similarity of the 3D structure of BsRacE with other proteins revealed that the most significant similarities are to the *Aquifex pyrophilus* MurI (28% sequence identity; see Figure 1), the similarities encompassing the majority of the fold and the spatial organization of both domains of the enzyme. In spite of this, there are important conformational changes between the two structures, having been suggested that the available structure of *Aquifex pyrophilus* MurI[21] represents a noncatalytic form of the enzyme.[18] In particular, in this solved structure of *Aquifex pyrophilus* MurI the side chain of His180 (His187 in BsRacE) is more than 7 Å from the thiol of the closest cysteine, Cys178 (Cys185 in BsRacE), and makes no contact with the substrate.

(18) Ruzheinikov, S. N.; Taal, M. A.; Sedelnikova, S. E.; Baker, P. J.; Rice, D. W. *Structure* **2005**, *13*, 1707.
(19) Tanner, M. E.; Gallo, K. A.; Knowles, J. R. *Biochemistry* **1993**, *32*, 3998.
(20) Spies, M. A.; Toney, M. D. *Biochemistry* **2003**, *42*, 5099.
(21) Hwang, K. Y.; Cho, C. S.; Kim, S. S.; Sung, H. C.; Yu, Y. G.; Cho, Y. J. *Nat. Struct. Biol.* **1999**, *6*, 422.
(22) Crooks, G. E.; Hon, G.; Chandonia, J.-M.; Brenner, S. E. *Genome Res.* **2004**, *14*, 1188.

In a preceding paper[23] we have carried out Molecular Dynamics simulations of the complex *Aquifex pyrophilus* MurI−D-glutamate with neutral Cys70 (Cys74 in BsRacE) and Cys178 (Cys185 in BsRacE) and an ionized Asp7 (Asp10 in BsRacE). Previously, Glu147′ (Glu153 in BsRacE) had protonated the substrate's α-carboxylate, according to the substrate activation mechanism proposed by Richard and co-workers[24,12] and supported by our calculations.[25] The results showed that Cys70 interacts with the side chain carboxylate oxygen of Asp7, the interatomic distance for many configurations being ∼4 Å or less, while Glu147′ interacts with His180 (the average interaction distance is 5.2 Å with a standard deviation of 1.2 Å). This fact indicates that, even starting from the available crystallographic structure of *Aquifex pyrophilus* RacE (solved when complexed with a substrate analogue, D-glutamine), once the system is conveniently activated, the population of the ensemble of configurations suitable to allow the mechanism involving two neutral cysteines and assisted by one aspartate and one histidine residue is possible. The stable existence of neutral cysteines agrees with the pK_a values that we obtained for the two cysteines in this ensemble: 13 and 13.5 for Cys70 and Cys178, respectively. However, such high pK_a values pose the question already mentioned above: In these conditions, how can Cys70 (D → L direction) or Cys178 (L → D direction) act as a catalytic base?

The purpose of this paper is to determine whether the four proton jumps mechanism involving two neutral thiols is feasible, focusing on the strategy used by glutamate racemase to make it possible in spite of the apparent extremely low capacity of both neutral cysteines for generating deprotonated cysteines at the reaction's pH. To this aim, we present here a theoretical study of the D-glutamate → L-glutamate reaction catalyzed by BsRacE, including Molecular Dynamics simulations with a Molecular Mechanics force field and a quite complete Quantum Mechanics/Molecular Mechanics (QM/MM)[26−28] exploration of the corresponding potential energy surfaces (PESs).

The *Bacillus subtilis* rather than the *Aquifex pyrophilus* species has been chosen in the present study because there is now more structural information of the reactive complex of the former,[18] which is a very relevant information for any theoretical study. Taking into account the available kinetic data for different RacE species,[29] it is reasonable to assume that the general catalytic mechanism could be common. However, these different species clearly differ in terms of quaternary structure, which in turn makes a substantial difference in the active site.[29] In *Aquifex pyrophilus*, the main chain carboxylate of the substrate in a given monomer interacts with the residue Glu147′ that belongs to the other monomer. As proposed by Rios et al.[12] and supported by our previous calculations,[25] Glu147′ activates the substrate by hydrogen transfer to it. However, the quaternary structure of *Bacillus subtilis* places the two actives sites of the biologically active dimer far from each other, and instead of a unique interaction, the substrate main chain carboxylate interacts with hydrogen donor groups of three residues that belong to the same monomer (as will be explained in the Results section). Thus, we propose that, in *Bacillus subtilis*, the proton transfer found in *Aquifex pyrophilus* to activate the substrate is substituted by these interactions, which contribute to stabilizing the carbanionic intermediate.

We want to emphasize that the glutamate racemase mechanism represents a very challenging problem not only from a chemical and biochemical point of view but also from the theoretical and computational side, as the transfer of four protons has to be taken into account.

2. Methods and Simulation Details

2.1. Initial Setup. Model of the Enzyme Complex. The initial structure was modeled from the 1.75 Å resolution X-ray crystal structure of the complex glutamate racemase-D-glutamate from the bacteria *Bacillus subtilis* with PDB code 1ZUW.[30] Although the crystals of BsRacE were grown in the presence of L-glutamate, the state of the electron density was consistent with its unambiguous assignment as D-glutamate.[18,30] This structure is therefore a good starting point to carry out a mechanistic study of the enzymatic reaction. The X-ray structure is composed by three monomers as a result of a crystallization artifact.[18] The enzyme is known to be biologically active as a dimer.[18] Chains A and C have been used for the setup, and chain B was discarded. The coordinates of the missing residues of the structure were automatically modeled with the ModLoop web server, which predicts the loop conformations by satisfaction of spatial restraints.[31,32] The coordinates of the hydrogen atoms of the protein and the substrate were determined using the HBUILD facility in the program CHARMM.[33] The protonation states of the titrable residues were assigned by the PROPKA[34] module of the PDB2PQR software package.[35] PROPKA is a very fast empirical method that is able to predict most protein pK_a values using information based on the position and chemical nature of the groups close to the pK_a sites. Most of the PROPKA predictions are within 1.0 pH units of the corresponding experimental values. Then, in spite of its empirical character, PROPKA can provide a useful estimation of the pK_a values. In all (including 1059 water molecules) the enzyme complex involves 11 749 atoms.

From this point, three diferent setups were performed to study the dynamical behavior of the enzyme and its reactivity. One setup was designed with the aim to carry out a classical Molecular Dynamics simulation (see section 2.2 for details), and the other two setups were designed in order to use a QM/MM potential to study the reactivity of the glutamate racemase enzyme.

The first QM/MM model contains 34 atoms in the QM region including the side chains of Asp10, Cys74, Cys185, and the substrate. The second QM/MM model is an extension of the first one including also His187 in the QM region with a total of 46 atoms. The QM/MM frontier has been treated with the generalyzed hybrid orbital (GHO) method.[36] The GHO atoms were the α-carbons of all the quantum residues. The structures were solvated with a 24 Å water sphere using the solvent-sphere.str script that can be found on the CHARMM forum[37] and choosing a minimal

(23) Puig, E.; Garcia-Viloca, M.; González-Lafont, A.; Lluch, J. M.; Field, M. J. *J. Phys. Chem. B* **2007**, *111*, 2385.
(24) Rios, A.; Richard, J. P. *J. Am. Chem. Soc.* **1997**, *119*, 8375.
(25) Puig, E.; Garcia-Viloca, M.; González-Lafont, A.; Lluch, J. M *J. Phys. Chem. A* **2006**, *110*, 717.
(26) Warshel, A.; Levitt, M. *J. Mol. Biol.* **1976**, *103*, 227.
(27) Singh, U. C.; Kollman, P. A. *J. Comput. Chem.* **1986**, *7*, 718.
(28) Field, M. J.; Bash, P. A.; Karplus, M. *J. Comput. Chem.* **1990**, *11*, 700.
(29) Lundqvist, T.; Fisher, S. L.; Kern, G.; Folmer, R.; Xue, Y.; Newton, D.; Keating, T.; Alm, R.; de Jonge, B. *Nature* **2007**, *447*, 817.
(30) Taal, M. A.; Sedelnikova, S. E.; Ruzheinikov, S. N.; Baker, P. J.; Rice, D. W. *Acta Crystallogr., Sect. D* **2004**, *60*, 2031.
(31) Fiser, A.; Do, R. K. G.; Sali, A. *Protein Sci.* **2000**, *9*, 1753.
(32) Fiser, A.; Sali, A. *Bioinformatics* **2003**, *18*, 2500.
(33) Brooks, B. R.; Bruccoleri, R. E.; Olafson, B. D.; States, D. J.; Swaminathan, S.; Karplus, M. *J. Comput. Chem.* **1983**, *4*, 187.
(34) Li, H.; Robertson, A. D.; Jensen, J. H. *Proteins* **2005**, *61*, 704.
(35) Dolinsky, T. J.; Nielsen, J. E.; McCammon, J. A.; Baker, N. A. *Nucleic Acids Res.* **2004**, *32*, W665.
(36) Gao, J.; Amara, P.; Alhambra, C.; Field, M. J. *J. Phys. Chem. A* **1998**, *12*, 4714.
(37) http://www.charmm.org/.

overlapping distance of 2.2 Å. For each setup the sphere was centered at the geometric center of the corresponding QM region.

The QM/MM PES was calculated by using the AM1 Hamiltonian for the QM region for the four proton transfers of the global mechanism that will be analyzed in detail in sections 3.2−3.4. However, the AM1-SRP (Specific Reaction Parameters) Hamiltonian developed by Major et al.[17] for the alanine racemase enzyme has also been used here to describe the two proton transfers involved in D-glutamate enantiomeric inversion (see section 3.3). The test calculations, included in Table S1 of the Supporting Information, on values of proton affinities for several model compounds show that the AM1 method gives acceptable values for the proton affinities of the conjugated basis of the following molecules in the gas phase: acetic acid (taken as a model of the aspartic residue, Asp10), ethanethiol (taken as a model of the cysteine residues Cys74 and Cys185), and protonated 4-methylimidazole (taken as a model of the protonated histidine residue, His187). So then, the AM1 model can be considered as a valid quantum model for describing the first step of the whole mechanism corresponding to the proton transfer from the thiol group of Cys74 to the Asp10 carboxylate, and also for describing the third step corresponding to the reprotonation of Cys185 by His187. However, the AM1 C_α proton affinity for the conjugated basis of alanine (zwitterion), taken as a model for D-glutamate substrate, is clearly underestimated in comparison with several DFT (Density Functional Theory) values.[17] In contrast, the AM1-SRP Hamiltonian of Major et al.[17] gives a more accurate value for the C_α proton affinity of the substrate model, and it is therefore a more quantitative approach for describing the deprotonation and reprotonation processes involving the C_α atom of D-glutamate and the two cysteines (Cys74 and Cys185). On the other hand, the reparametrized semiempirical method might not be well-balanced and several convergence problems of the quantum wave function have been encountered on different regions of the QM(AM1-SRP)/MM PES for the D-glutamate racemase enzyme. The CHARMM22 force field was used for the MM part.[38] Water molecules were modeled with the TIP3P[39] potential.

The QM/MM van der Waals interactions were recalibrated. The CHARMM22 van der Waals parameters are expected to work between MM atoms belonging to this force field, but they may not describe correctly an MM−QM(AM1) interaction. The new parameters were used in our previous QM/MM works on glutamate racemase and were obtained following the procedure described by Freindorf and Gao.[40] We have considered the complexes of water with models of the cysteine, histidine, and aspartic side chains in different protonation states, together with a model of the substrate's ammonium group (see Supporting Information). Table S2 provides the total interaction energies of the complexes at the Hartree−Fock level and also using QM/MM calculations with the van der Waals parameters obtained from the CHARMM force field, from Freindorf and Gao and co-workers,[41] or after our optimization procedure. The optimization parameters are shown in Table S3.

The initial structure for the QM/MM surface explorations was prepared as follows. The solvated complex was minimized using the Adapted Basis Newton−Raphson (ABNR) algorithm for 40 steps keeping the QM part fixed. Then a leapfrog Langevin Molecular Dynamics simulation was carried out for 10 ps with the protein and the substrate atoms fixed and moving just the water molecules.

The first QM/MM model was used to study the protonation of the Asp10 residue by Cys74 (see section 3.2). The solvated complex was gently heated up to 100 K during 100 ps of a Molecular Dynamics simulation using stochastic boundary conditions as described in section 2.2. Then, the mobile part of the system was minimized until a gradient tolerance of 0.01 kcal/(mol Å) was reached. After performing the PES exploration for the first proton transfer, we decided to include the His187 residue also in the QM part. The system was again minimized until a gradient tolerance of 0.01 kcal/(mol Å) was reached. With this second QM/MM model the enantiomeric inversion (see section 3.3) and the reprotonation of Cys185 by His187 were studied (see section 3.4).

2.2. Molecular Dynamics Simulation. As mentioned above (see section 2.1), the first setup was created with the aim to carry out a Molecular Dynamics study. As explained in the same section, the system was solvated with a 24 Å water sphere. The water molecules were minimized for 40 steps with the ABNR algorithm, and 2.5 ps of Molecular Dynamics were carried out at 300 K, keeping the protein and substrate atoms fixed, to allow the water molecules to relax.

The solvated system was then minimized for 60 steps keeping fixed all the atoms outside the water sphere. Stochastic boundary conditions were used to mimic the aqueous environment. The system was divided into three zones: (1) the reaction zone, from the origin to 20 Å, where all atoms included in this zone are treated with Newtonian dynamics; (2) the buffer zone, from 20 to 24 Å, where all atoms are treated with Langevin dynamics; and (3) the reservoir zone, where all atoms were fixed. The protein atoms were assigned to one or another region according to the reference structure at the beginning, and they retained their labels during the simulation. Water molecules were allowed to diffuse between the reaction zone and the buffer zone. The Langevin dynamics regime imposes a friction coefficient and a random force on the heavy atoms in the buffer region. The harmonic force constants were taken as 1.22 kcal/(mol Å^2) for the main chain O atoms, 1.30 kcal/(mol Å^2) for all other main chain atoms, and 0.73 kcal/(mol Å^2) for side chain atoms and water molecules. The friction constants were 200 ps^{-1} for the protein atoms and 62 ps^{-1} for the water atoms in the buffer region. A deformable boundary potential was imposed on water molecules at the buffer/reservoir interface to represent the effect of bulk solvent outside this boundary.

The solvated system was gradually heated up to 300 K during 300 ps and then was equilibrated during 800 ps. From the final structure we ran a simulation for 7 ns, saving structures at every 500 steps with a time step of 1 fs. The equations of motion were propagated using the leapfrog integrator. In the present study a cutoff of 13.5 Å was used along with a switching function in the region from 12.0 to 13.5 Å to smoothly reduce the interactions to zero. The nonbonded pair list was updated every 25 steps. All bond lengths involving hydrogen atoms were constrained by the SHAKE algorithm.[42]

2.3. Reaction Coordinates and Optimization Details. Reduced potential energy profiles of the different proton transfers that compose the global enzymatic reaction have been generated. Figure 2 shows schematically the atoms of the catalytic residues involved in each proton transfer.

The first reaction studied corresponds to the proton transfer from Cys74 to Asp10. The reaction coordinate used to define this 1D-profile is the antisymmetric combination of distances involving the sulfur of the Cys74 residue (Cys74-*Sγ*), the proton bonded to it (Cys74-*Hγ*), and one of the oxygens of the Asp10 carboxylate (Asp10-*Oδ*1). This reaction coordinate is labeled RC_{CD}; the CD subscript indicates that the proton is driven from the Cysteine (C) to the Aspartate (D).

$$RC_{CD} = r_{C74S\gamma-C74H\gamma} - r_{C74H\gamma-D10O\delta1} \quad (1)$$

Once the Cys74 sulfur is deprotonated the enantiomeric inversion of the glutamate is ready to be explored. In order to study it, two reaction coordinates are defined. RC_{dep} describes the deprotonation

(38) Mackerell, A. D., Jr. *J. Phys. Chem. B* **1998**, *102*, 3586–3616.
(39) Jorgensen, W. L.; Chandrasekhar, J.; Madura, J.; Impey, R. W.; Klein, M. L. *J. Chem. Phys.* **1983**, *79*, 926.
(40) Freindorf, M.; Gao, J. *J. Comput. Chem.* **1996**, *17*, 386.
(41) Xia, X.; Gao, J. *Science* **1992**, *258*, 631.
(42) Ryckaert, J.-P.; Ciccotti, G.; Berendsen, H. J. C. *J. Comput. Phys.* **1977**, *23*, 327.

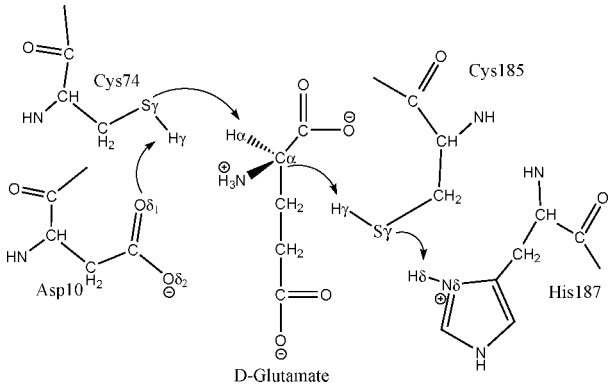

Figure 2. Schematic representation of the active site and the reaction mechanism.

of the Hα of the substrate and involves the sulfur of Cys74, the α-proton, and the α-carbon atoms of the substrate.

$$RC_{dep} = r_{H\alpha-C\alpha} - r_{C74S\gamma-H\alpha} \quad (2)$$

The RC_{prot} reaction coordinate is defined as the antisymmetric combination of distances involved in the protonation of the α-carbon by the γ-proton of Cys185.

$$RC_{prot} = r_{C185S\gamma-C185H\gamma} - r_{C185H\gamma-C\alpha} \quad (3)$$

Finally, the reprotonation of the Cys185 by His187 is studied with a 1D-profile with another antisymmetric combination of distances involving the δ-proton and the δ-nitrogen of His187 and the Cys185 sulfur.

$$RC_{HC} = r_{N\delta-H\delta} - r_{H\delta-C185S\gamma} \quad (4)$$

1D and 2D scans have been obtained by a series of geometry optimizations of the mobile part of the system in the presence of harmonic restraints applied on the different reaction coordinates previously defined. The RESD module in CHARMM was used to define the harmonic restraint terms of the form

$$V_{RESD} = \frac{1}{2}k_{RESD}(RC - RC_{REF})^2 \quad (5)$$

where k_{RESD} is the restraining force constant, which was set equal to 2500.0 kcal/(mol Å^2). The quantity RC_{REF} is the reference value of the reaction coordinate at each energy minimization calculation. Each minimization was carried out with a gradient tolerance of 0.01 kcal/(mol Å) with the ABNR algorithm. In these minimizations the reaction coordinate was projected out of the gradient. All the atoms 24 Å away from the center of the active site were kept frozen during the optimizations.

The conjugate peak refinement (CPR) algorithm[43] was used to find a smooth reaction path. Optimized structures from the 2D-PES were used as input for the CPR algorithm. The mobile part of the system and the electrostatic cutoff were the same as those in the RESD minimizations. The CPR path has been displayed along the coordinate RC4 defined as follows.

$$RC4 = RC_{prot} + RC_{dep} \quad (6)$$

3. Results and Discusion

3.1. Molecular Dynamics Simulations. As mentioned above, Molecular Dynamics simulations of the reactant structure of the enzyme/substrate complex have been carried out for 7 ns. During this simulation the distances between the atoms that will be involved in each of the successive proton transfers in the mechanism proposed were monitored, and the interactions that the catalytic residues and the substrate can form have been analyzed.

The first step corresponds to the transfer of a proton from the thiol group of the Cys74 to the Asp10 carboxylate. The evolution of the distance between the Asp10-$O\delta1$ atom and the Cys74-$S\gamma$ atom is shown in Figure 3A. At the beginning of the simulation they are far from each other (∼5 Å). However, the distance decreases during the first 1.5 ns until a hydrogen bond is formed between those two atoms. This distance fluctuates mostly within the range 3−4.5 Å for the next 5 ns. The average distance along the 7 ns turns out to be 3.91 Å, and the occupancy of this hydrogen bond is 0.24. The occupancy stands for the fraction of the configurations that hold the hydrogen bond, and here it is determined as follows: The generated configurations have been analyzed every 5 ps, and one analyzed configuration is counted as involving a hydrogen bond if the distance between the corresponding hydrogen atom and the acceptor heavy atom is less than 2.4 Å, and this situation is maintained at the next analyzed configuration 5 ps later. These results show that the sulfur of Cys74 and the oxygen of the carboxylate of Asp10 can therefore approach each other quite easily, so that the region of configurations able to produce the first proposed proton transfer are repeatedly visited. The oscillation of the distance between Cys74 and Asp10 occurs thanks to the mobility of the side chain of Cys74 which is thus able to establish this hydrogen bond with Asp10 during all of the simulation. Conversely, the side chain of Asp10 is fixed by strong hydrogen bonds between the two oxygen atoms (Oδ1 and Oδ2) of its carboxylate and two strictly conserved residues, Ser11 (occupancy 0.93) and Thr186 (occupancy 0.91), respectively. Asp10 also interacts through a salt-bridge interaction with the ammonium group of the substrate which in this hydrophobic pocket (see Figure 1) produces a stabilization of the system. Then, Asp10 interacts with both Cys74 and the substrate already orienting and preparing them for the next proton transfer as will be seen later.

The second step involves both the deprotonation of the substrate's α-carbon by the Cys74-$S\gamma$ and the reprotonation of that carbon atom by the Cys185-$S\gamma$ (see below for a discussion of the concertedness of both proton transfers). The evolution of the corresponding distances along the reactant complex simulation is also displayed in Figure 3B and 3C, respectively. The distance between the sulfur atom of Cys74 and the α-carbon of the substrate fluctuates along the 7 ns mostly from 3.3 Å to 4.5 Å (the average distance is 3.82 Å, with an occupancy value of 0.00). The sulfur atom is always kept at a distance close enough to begin the abstraction of the substrate's Hα although the corresponding hydrogen bond is never formed due to the fact that the thiol group of Cys74 is still protonated. From comparison of Figure 3A and 3B, it is worth noting that the sulfur atom of Cys74 is very seldom closer than 3.4 Å to both the oxygen of the carboxylate of Asp10 and the α-carbon of the substrate at once. In contrast, the second cysteine is at a larger distance from the substrate. The average distance between the Sγ atom of Cys185 and the substrate's Cα is ∼5.66 Å (as expected, the occupancy is 0.00) and fluctuates mostly from 4.6 to 6.6 Å. However, this distance is expected to be easily reduced when the deprotonation of the substrate begins and the Cα becomes negatively charged. The side chain of Cys185 can easily reorient as the sulfur atom does not interact significantly with any residue during all the simulations.

The last step consists of the reprotonation of Cys185 by His187. The change of the distance between the Sγ atom of

(43) Fischer, S.; Karplus, M. *Chem. Phys. Lett.* **1992**, *194*, 252.

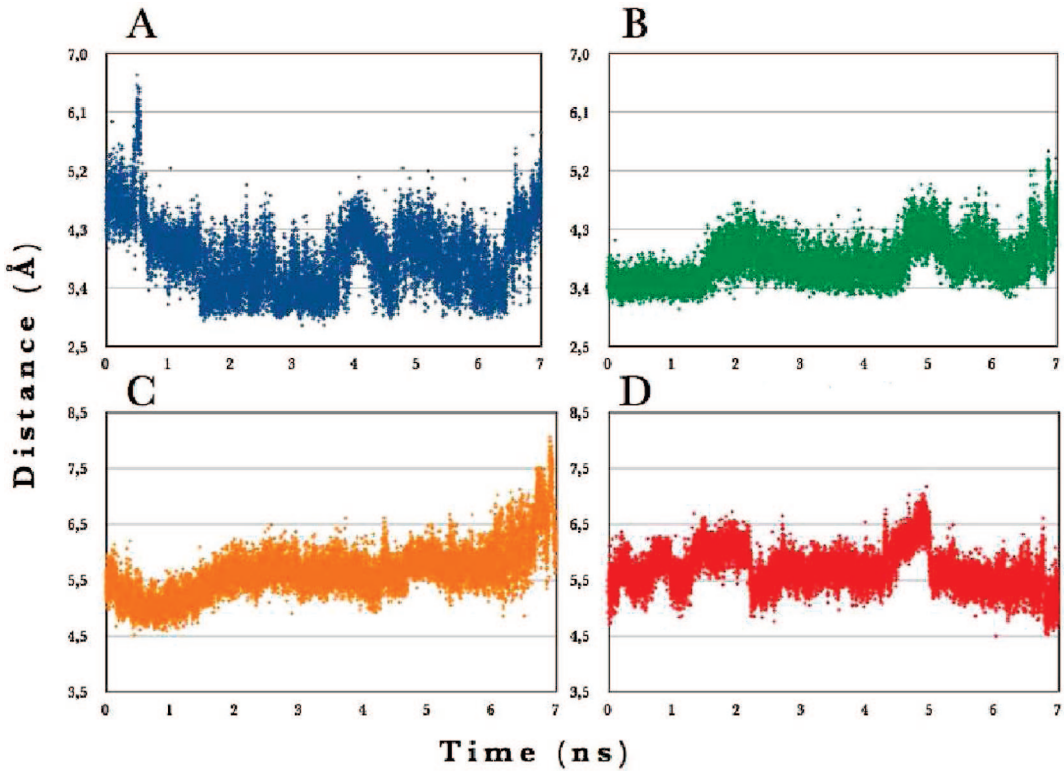

Figure 3. (A) Evolution of the distance between atoms Asp10-*Oδ*1 and Cys74-*Sγ*. (B) Evolution of the distance between atoms Cys74-*Sγ* and D-Glu-*C*α. (C) Evolution of the distance between atoms Cys185-*Sγ* and D-Glu-*C*α. (D) Evolution of the distance between atoms Cys185-*Sγ* and His187-*Nδ*.

Cys185 and the Nδ atom of His187 is displayed in Figure 3D. This distance fluctuates mostly within the range 4.6−6.6 Å, with an average value of 5.70 Å (of course, the occupancy is 0.00). This distance would be reduced once Cys185 is negatively charged. The acid/base behavior of His187 strongly depends on its interaction with another strictly conserved residue, Glu153. The corresponding distance between the Nε atom of His187 and the Oε2 of Glu153 fluctuates a lot along the simulation (with an average value of 5.40 Å), but forming a hydrogen bond for a long period of more than 1.5 ns (occupancy of 0.24 along the 7 ns of the simulation).

An analysis of the substrate's interactions along the simulation reveals that D-glutamate is able to form hydrogen bonds with many residues of the enzyme through its side chain carboxylate, its ammonium group, and specially through its α-carboxylate. The average distances between the heavy atoms involved in the hydrogen bonds, along with the corresponding occupancies, are given in Table 1. There are three residues that solvate the α-carboxylate of the substrate forming hydrogen bonds with it by their side chains and/or their backbone HN proton. The strictly conserved Asn75 residue interacts through its side chain $H\delta 2_2$ atom with the substrate's Oτ2 with an occupancy of 0.84. Besides, its backbone HN proton is able to interact with both oxygen atoms of the substrate's carboxylate with occupancies of 0.61 (Oτ1) and 0.77 (Oτ2), respectively. The next residue in the sequence of amino acids, Thr76, is also a strictly conserved residue and interacts with the substrate's Oτ2 through its side chain hydroxyl with an occupancy of 0.54. The third residue interacting with this substrate's carboxylate is Thr186. This residue is also strictly conserved and is found between the catalytic residues Cys185 and His187. Thr186 hydrogen bonds to the substrate's Oτ2 with its backbone HN proton, with an occupancy of 0.83. Its Oγ also forms a hydrogen bond with the substrate's NH_3^+ group, the occupancy being 0.93 (in the case of interactions between the NH_3^+ group and the enzymatic residues, a hydrogen bond is considered to exist when any of the NH_3^+ hydrogens fulfills the criterion defined above for the occupancy). Another very important hydrogen bond, which has already been mentioned above, exists between the substrate's NH_3^+ group and the Oδ1 atom of the side chain carboxylate of Asp10. It has to be remembered that, before the set of proton transfers occur, Asp10 is still deprotonated, so that its Oδ1 atom holds a net negative charge. In this sense, the hydrogen bond (with an occupancy of 0.86) with the NH_3^+ of D-glutamate efficiently contributes to the stabilization of the ionized Asp10.

Table 1. Most Important Hydrogen Bond Interactions of the Substrate along the MD Simulation[a]

$Atom_1$	$Atom_2$	occupancy	average distance (Å)
		D10	
NH_3^+	$O\delta_1$	0.86	2.82 ± 0.35
		S11	
$O\varepsilon_2$	Hγ	0.51	3.86 ± 1.35
		N75	
$O\tau_2$	$H\delta_{2_2}$	0.84	3.01 ± 0.30
$O\tau_1$	HN	0.61	3.03 ± 0.23
$O\tau_2$	HN	0.77	3.16 ± 0.33
		T76	
$O\tau_2$	Hγ	0.54	3.15 ± 0.53
		T186	
NH_3^+	Oγ	0.93	2.83 ± 0.14
$O\tau_2$	HN	0.83	3.08 ± 0.31

[a] $Atom_1$ is the atom corresponding to the substrate, and $Atom_2$ is the atom corresponding to the enzymatic residue. For NH_3^+, no distinction is made between the hydrogen atoms to calculate the occupancy values.

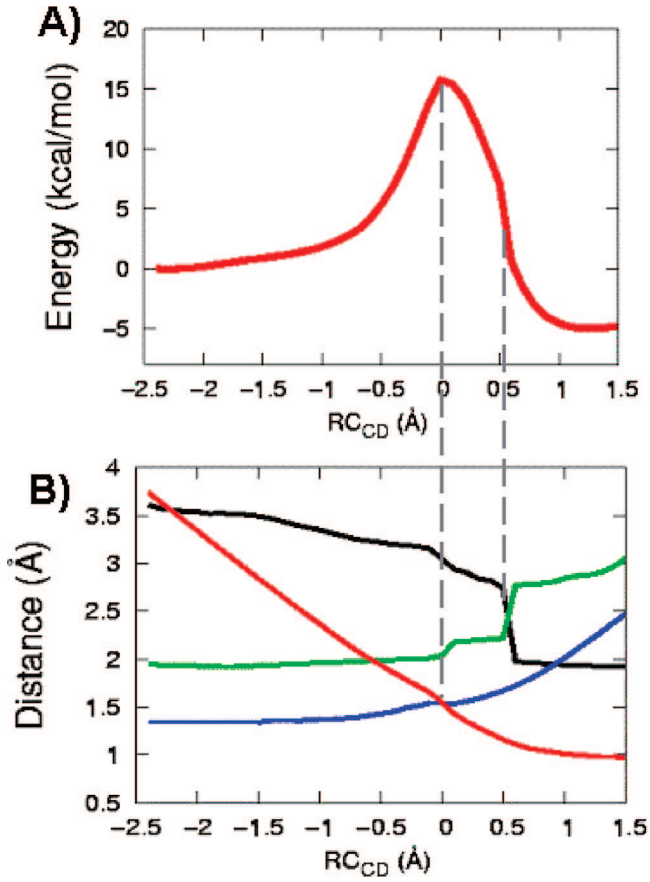

Figure 4. (A) Energy profile of the protonation of Asp10-$O\delta$ 1 by Cys74-$S\gamma$. (B) Evolution of the most relevant atomic distances along the RC_{CD} coordinate. Black: Hτ2 and Cys74-$S\gamma$. Green: Hτ2 and Asp10-$O\delta$1. Red: Cys74-$H\gamma$ and Asp10-$O\delta$ 1. Blue Cys74-$H\gamma$ and Cys74-$S\gamma$.

All these conserved residues in the active site have two major roles. On one hand, they orient and bind the substrate in the active site. The D-glutamate ligand anchors the polar active site residues maximizing its interactions with them. On the other hand, these residues strongly solvate the substrate's α-carboxylate group and delocalize the negative charge that supports the substrate once the carbanionic species is generated.

The most important result that arises from the Molecular Dynamics simulation is that the enzyme/D-glutamate Michaelis complex is ready to undergo the first proton transfer that will initiate the conversion of D-glutamate to L-glutamate. Moreover, the arrangement and the capacity of motion of the different residues around the substrate in the active site seem to be adequate to allow the successive reorganizations required to make possible the subsequent proton transfers that will complete the mechanism.

3.2. First Proton Transfer: From Cys74 to Asp10. The potential energy profile corresponding to the proton transfer from the Sγ atom of Cys74 to the Oδ1 atom of the carboxylate of Asp10 as a function of the reaction coordinate RC_{CD} is displayed in Figure 4A on the QM(AM1)/MM PES. To reduce hysteresis effects, the coordinate RC_{CD} was explored forward, backward, and forward again. This figure shows the final second forward exploration. The negative values of the reaction coordinate correspond to the reactant region, when the shifting proton (Hγ) is still closer to the donor sulfur atom than to the acceptor oxygen atom, thus involving a neutral Cys74 residue and a negative Asp10. On the other hand, the evolution of the most relevant distances along the reaction coordinate is shown in Figure 4B: the distances between the transferring proton and the donor and acceptor atoms, and the distances between the proton Hτ2 of the D-glutamate ammonium group and both the Asp10-$O\delta$ 1 and the Cys74-$S\gamma$. At the beginning of the proton transfer the energy profile is nearly flat. From $RC_{CD} = -2.5$ Å to $RC_{CD} = -1$ Å, the energy just increases 1.8 kcal/mol. In this region the side chain of Cys74 (recall the mobility exhibited by this side chain during the Molecular Dynamics simulations) easily approaches Asp10, producing a very important shortening of the Hγ−Oδ1 distance and a slight diminution of the Hτ2−Sγ distance, although the breakage of the Hγ−Sγ bond has not begun yet.

As the Cys74 side chain becomes closer and closer to Asp10, the compression of the Hγ against the Oδ1, initiating the formation of the new bond, causes an abrupt rise of the potential energy curve, whose maximum is reached just when the Hγ−Oδ1 and Hγ−Sγ distances become equal at $RC_{CD} = 0$ Å (however, taking into account the different lengths of the equilibrium internuclear distances corresponding to the S−H and O−H bonds, at this point the Hγ−Sγ bond is still more formed than the Hγ−Oδ1 one). The corresponding potential energy barrier turns out to be 15.8 kcal/mol. From that point, as the formation of the new bond and the cleavage of the old bond advance, already in the positive region of RC_{CD}, the potential energy decreases. At $RC_{CD} = 0.55$ Å, when the Hγ−Oδ1 bond is already almost entirely formed, the potential energy is still roughly 5 kcal/mol above the reactants. From this point, an additional stabilization of ∼10 kcal/mol occurs, in such a way that the proton transfer from Cys74 to the Asp10 turns out to be energetically favored by 5.0 kcal/mol in terms of potential energy. This stabilization can be mainly attributed to the change in the interactions between the D-glutamate ammonium group and these two residues that accompanies the proton transfer. At the reactants, the positive ammonium's substrate group interacts with the negatively charged Asp10. Once the Asp10 gets the proton from Cys74, this salt-bridge interaction is lost and the ammonium group approaches the nascent deprotonated Cys74 residue to form another salt-bridge interaction. This new interaction with the cysteine is stronger than that with the aspartate as the negative net charge is now more localized on the sulfur atom of the cysteine, whereas before it was delocalized between the two carboxylate oxygens of Asp10. Furthermore, before the proton transfer, Asp10 hydrogen bonds to several residues surrounding it and a water molecule, which also contribute to delocalize the initial negative net charge. In contrast, after the proton transfer, the negative charge is only localized on the sulfur atom of the anionic Cys74. As seen in Figure 4B, the flip of the ammonium group during the proton transfer occurs suddenly at $RC_{CD} = 0.5-0.6$ Å, so provoking a drastic decrease of the potential energy. Thus the electrostatic interactions of the substrate's ammonium group modulate the relative thermodynamic stability of the reactants and products of this first proton transfer. In the absence of this contribution, the shifting proton would easily revert to Cys74, which would be then unable to capture the α-proton of the substrate.

To confirm the influence of the substrate in the acidity of the residues involved in this proton transfer, pK_a calculations using PROPKA including and excluding the substrate were performed before proton transfer occurs. The pK_a of Cys74 when the substrate is included decreases from 9.75 to 6.23 (a notorius change taking into account that the substrate's ammonium group is not now close to Cys74, but to Asp10, and that Cys74 is still

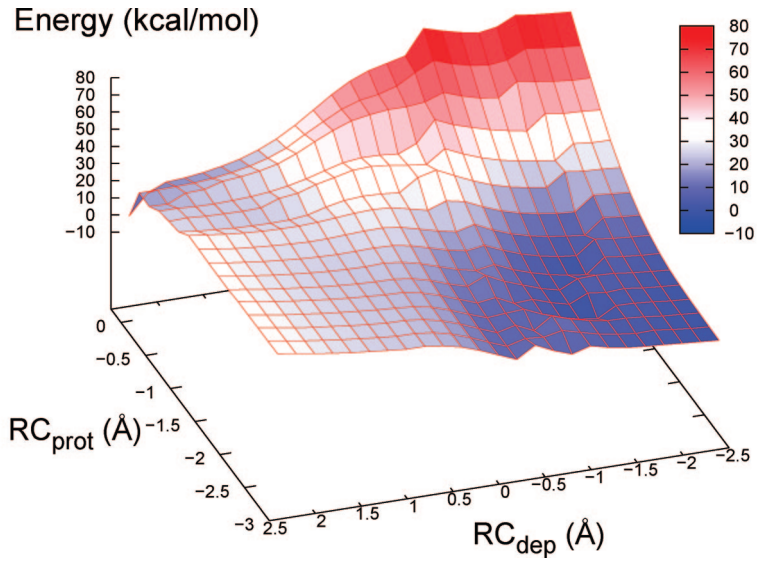

Figure 5. Bidimensional QM(AM1)/MM PES of the enantiomeric inversion.

neutral). This difference in pK_a is mainly due to the long-range electrostatic interaction with the positive net charge on the substrate's ammonium group. A similar trend is observed with the Asp10 residue. Its pK_a decreases from 5.53 to 2.52 when the substrate is included. Therefore, Asp10 is too acidic to get the proton from Cys74 while it is interacting with the ammonium group of D-glutamate. However, when this interaction is lost due to distance fluctuations and the ammonium group approaches Cys74-$S\gamma$ atom, Asp10 and Cys74 become less and more acidic, respectively, and the proton transfer may take place. As a matter of fact, it can be said that the jump of the ammonium group and the proton transfer happen in a concerted and coupled way.

It is interesting to note that Asp10 undergoes the most strong desolvation effect in the enzyme according to the PROPKA calculations (the desolvation effect is determined by assessing how many protein atoms are within a given distance of the ionizable residue). pK_a calculations from selected snapshots of the Molecular Dynamics simulations (see section 2.2) present a positive ΔpK_a ranging from 4 to 6 units due just to this effect. The precise location of this residue in the hydrophobic pocket of the enzyme enables the deprotonated Asp10 to act as a base and be able to deprotonate Cys74. Moreover the acid/base behavior of this residue can be modified by its interactions with the substrate.

3.3. Enantiomeric Inversion. Once the Cys74 residue is deprotonated, it is ready to abstract the Hα atom from the D-glutamate. Now the first point to be considered is whether the reprotonation of the α-carbon atom of the carbanionic intermediate by Cys185 occurs within the same step or not.

The bidimensional QM(AM1)/MM PES built as a function of RC_{dep} and RC_{prot} is displayed in Figure 5. The reaction coordinates evolve from negative to positive values as the deprotonation and reprotonation processes, respectively, advance (see eqs 2 and 3). As expected, a pathway consisting of a first protonation and then the deprotonation would imply a huge energy cost and can be dismissed. Instead, the opposite order is much less expensive, although in this case a wide range of quasi-degenerate reaction pathways exist as a consequence of the flatness of the PES in this region. Then, the first and last structures (that is, going from reactants to products) of the grid used to built the PES were further minimized with no restraints to obtain structures corresponding to the reactant and the product of the enantiomeric inversion. These two structures were used to obtain the conjugate peak refinement (CPR) path shown in Figure 6A (green line) as a function of the coordinate RC4, which takes into account both processes (deprotonation and reprotonation) at once. The resulting one-dimensional potential energy profile presents a first maximum (RC4 $\simeq -4.5$ Å), an intermediate minimum (RC4 $\simeq -3.8$ Å), and a second maximum (RC4 $\simeq 0$ Å) with a potential energy barrier of $\sim$18 kcal/mol, which is a really low energy barrier taking into account that a cysteine is deprotonating a very low acidic proton such as the Hα of D-glutamate.

As mentioned in section 2.1, the two proton transfers involved in the enantiomeric inversion process have also been studied using the QM(AM1-SRP)/MM potential. However, the corresponding bidimensional PES could not be calculated due to convergence problems of the AM1-SRP wave function at several geometries of the grid defined by RC_{dep} and RC_{prot} values. For this reason, only a CPR path (shown as a red line in Figure 6A) could be obtained on the QM(AM1-SRP)/MM PES for the enantiomeric inversion step. The first and last structures used to calculate this second CPR path were obtained by minimizing without restraints on the QM(AM1-SRP)/MM PES. The initial guesses for that optimization have been the reactant and product optimized geometries of the QM(AM1)/MM CPR. It can be observed that the QM(AM1-SRP)/MM CPR has only one maximum located at around RC4 = 0 Å, like the second maximum on the QM(AM1)/MM CPR, but with an energy barrier of 23.7 kcal/mol, nearly 6 kcal/mol higher than with the AM1 model. However, as mentioned in section 2.1, the AM1 Hamiltonian has severe problems in reproducing the Cα-proton affinity for the conjugated basis of alanine (zwitterion) (taken as a model for D-glutamate substrate). In fact, the AM1 value for that Cα proton affinity is $\sim$23 kcal/mol lower than the values calculated at higher levels of electronic structure theory.[17] For this reason, we believe that the AM1-SRP model is a better semiempirical parametrization for this region of the PES, and from now on, only the results of the QM(AM1-SRP)/MM approach will be given in this section.

The structure of the QM(AM1-SRP)/MM CPR maximum is depicted in Figure 7. The existence of only one maximum along the reaction path clearly indicates that the two proton transfers

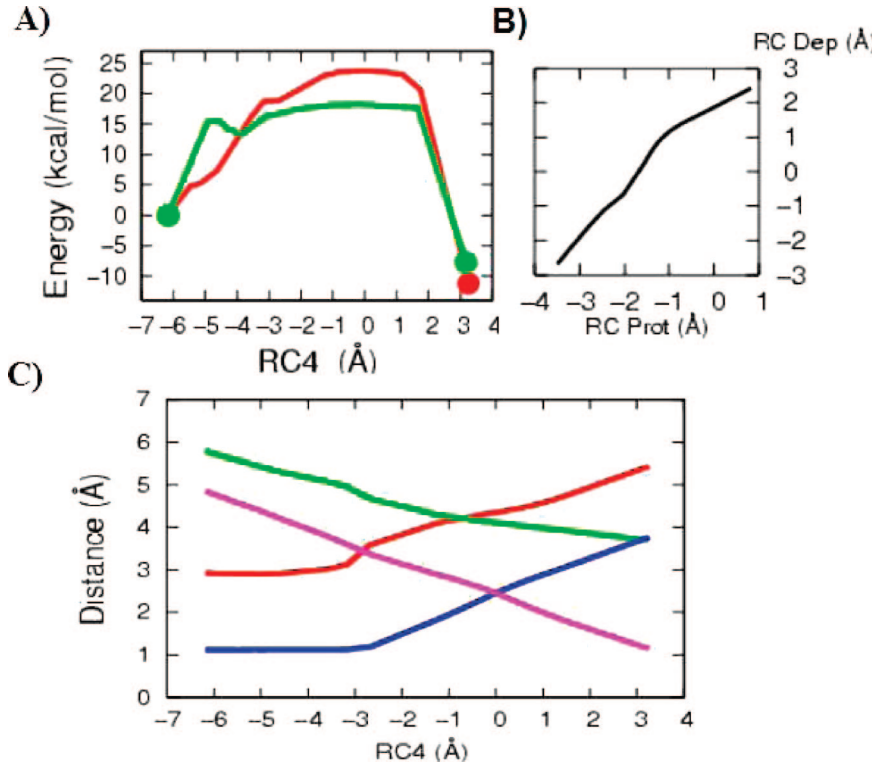

Figure 6. (A) Potential energy along the CPR path versus the RC4 coordinate: QM(AM1)/MM in green, QM(AM1-SRP)/MM in red. As explained in the text, the first and last structures of the QM(AM1)/MM path have been obtained by minimizing two structures of the grid used to build the PES shown in Figure 5. The CPR method has been used to connect both extremes (marked by two green dots). These structures were further minimized with the QM(AM1-SRP)/MM potential (marked also by two dots), and the red CPR path was located. (B) Projection of the QM(AM1-SRP)/MM CPR path on RC_{prot} and RC_{dep} coordinates. (C) Most relevant atomic distances involved in the enantiomeric conversion along the QM(AM1-SRP)/MM path. Red: Between atoms Cys74-$S\gamma$ and D-Glu-N. Green: Cys185-$S\gamma$ and D-Glu-N. Blue: D-Glu-Hα and D-Glu-Cα. Purple: Cys185-Hγ and D-Glu-Cα.

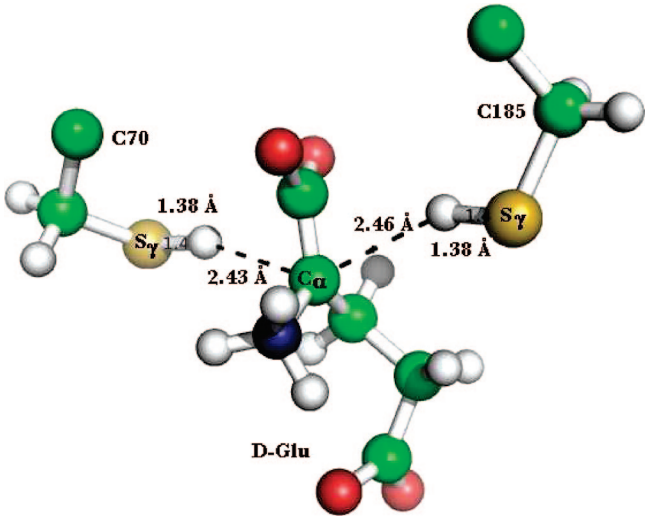

Figure 7. CPR saddle point geometry on the QM(AM1-SRP)/MM potential during the enantiomeric inversion.

take place in a concerted way on the PES. However, the deprotonation and reprotonation of the substrate by Cys74 and Cys185, respectively, take place in a highly asynchronic way. The distances of Cys74-Sγ with respect to the leaving (deprotonation) proton and of Cys185-Sγ with respect to the incoming (reprotonation) proton are both 1.38 Å, somewhat longer than the covalent S−H distance of a cysteine (1.33 Å). These values clearly indicate that at the region of the saddle point the deprotonation process has nearly finished when the reprotonation process has just initiated. In agreement, it can be observed that the distances between the α-carbon and the leaving and incoming protons (2.43 and 2.46 Å, respectively) are very long. The similarity between both Sγ-H and both Cα-H distances reflects the symmetrical disposition of the two cysteines with respect to the α-carbon of D-glutamate at the region of the saddle point.

The asynchronic character of this double proton transfer can also be asserted from the results shown in Figure 6B, in which the CPR path has been decomposed in both RC_{dep} and RC_{prot}. The structure of the CPR maximum is located at $RC_{dep} = 1.0$ Å and $RC_{prot} = -1.0$ Å. The positive value of RC_{dep} indicates again that the deprotonation process is quite advanced, whereas the negative sign of RC_{prot} means that the reprotonation process is just beginning. On the other hand, the evolution of the most relevant distances along the reaction coordinate RC4 is shown in Figure 6C: the distances between the α-carbon and the leaving (deprotonation) and incoming (reprotonation) protons, and the distances between the nitrogen of the D-glutamate ammonium group and both Cys74-$S\gamma$ and Cys185-$S\gamma$ atoms. In Figure 6C, it can also be verified that the region where the two C−H distance curves cross each other corresponds nearly to RC4 = 0 Å and that this crossing distance is long enough to say, as already inferred from Figure 7, that deprotonation has almost been completed before the reprotonation begins. Before that region, for RC4 values from −7 to −3 Å approximately, the increase of potential energy along the CPR path (see Figure 6A) correlates with a decrease in distance between the incoming proton and the α-carbon, as shown in Figure 6C. In any case, Cys185 is still very far from the substrate in that region, and as the distance between the α-carbon and the leaving proton does

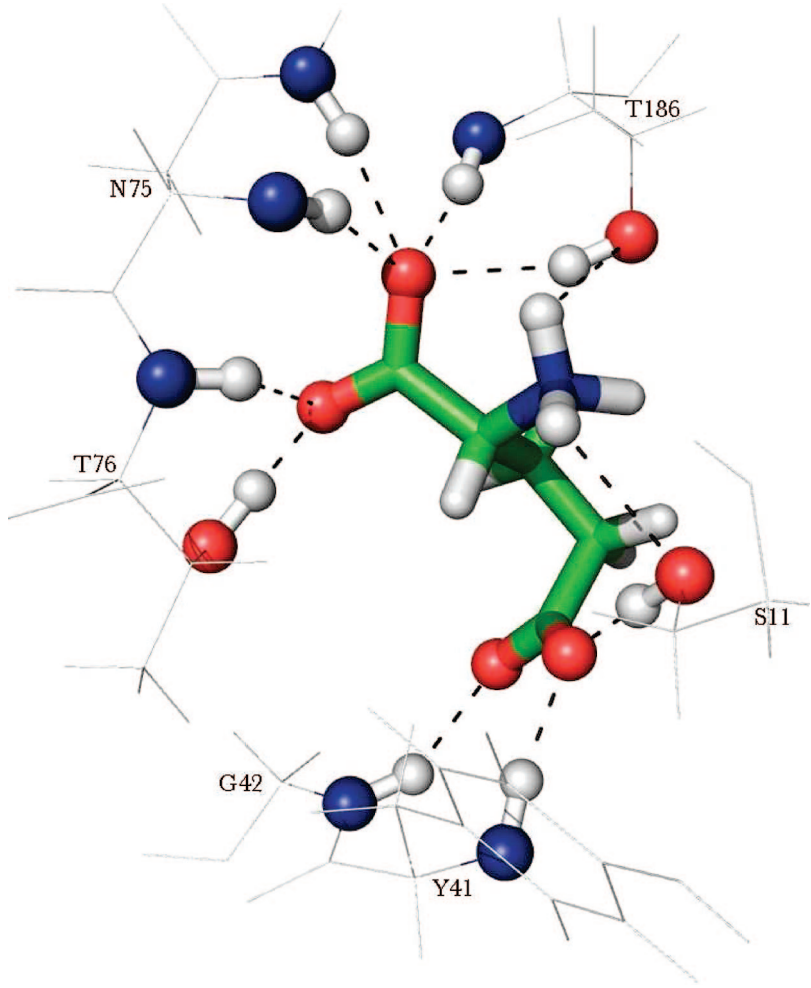

Figure 8. Hydrogen bond interactions of the substrate in the active site of the enzyme.

not change, it is also obvious that the deprotonation process has not begun yet. It is at around RC4 = −2.75 Å that the deprotonation process really begins because the H(leaving)−Cα distance begins to increase (see Figure 6C). The final uphill increase (just before the saddle point region) of potential energy is noticeable in Figure 6A and correlates with the deprotonation process. After the saddle point region, when the substrate is being reprotonated by Cys185 (at $RC_{prot} \simeq 0$ Å), RC_{dep} is already at 2 Å. At this point RC4 is 2.0 Å, and Figure 6C shows that whereas the formation of the new Cα−Hα bond is quite advanced, the original Hα−Cα is fully broken. So, the analysis of the results shown in Figures 6 and 7 permits us to conclude that deprotonation precedes reprotonation. So then, the enantiomeric inversion occurs in a concerted manner, although highly asynchronic. Interestingly, the theoretical result obtained recently by Stenta et al.[44] for the enantiomeric inversion between L- and D-proline catalyzed by the related enzyme proline racemase indicates a highly asynchronic concerted process, which confirms the hypothesis that Albery and Knowles wrote from the results of their work on this enzyme.[45] Altogether, these results support the idea of a common mechanism for the PLP independent enzymes.[8]

BsRacE does not use any cofactor such as PLP to acidify the Hα. This cofactor attaches the ligand by acting as an electron sink. To produce a similar effect, the glutamate racemase enzyme is able to create a strong hydrogen bond network (see Figure 8) solvating the substrate α-carboxylate, which aids delocalizing the negative charge developed once the Hα has been abstracted (remember that α-carbon deprotonation precedes reprotonation). This nascent negative net charge is also stabilized by the neighboring positive charge of the ammonium group of the substrate. Quite interestingly, in Figure 6C it can be seen that the increase of the distance between the D-glutamate ammonium group and the Cys74-$S\gamma$ atom parallels the evolution of the Hα−Cα distance corresponding to the deprotonation process, while, in turn, the decrease of the distance between the D-glutamate ammonium group and the Cys185-$S\gamma$ atom parallels the evolution of the new C−H distance corresponding to the reprotonation process. That is, the ammonium group of the substrate moves during the deprotonation/reprotonation processes as the negative net charge migrates from Cys74 to Cys185, accompanying and facilitating both proton transfers. The crossing of the two distances of the D-glutamate ammonium group to the Cys74-$S\gamma$ and the Cys185-$S\gamma$ atoms appears very close to the crossing between the two C−H distances.

The pK_a values of the cysteines are also perturbated by the desolvation effect caused by this buried active site. The Cys74 residue is the fifth most desolvated residue of the protein with a ΔpK_a of up to +3.4 units (according to the PROPKA results). Thus, the acidity of Cys74 is decreased to deprotonate the Cα. The acid/base behavior of Cys185 depends in a very important

(44) Stenta, M.; Calvaresi, M.; Alto, D.; Garavelli, M.; Bottoni, A *J. Phys. Chem. B* **2008**, *112*, 1057.
(45) Albery, W. J.; Knowles, J. R. *Biochemistry* **1986**, *25*, 2572.

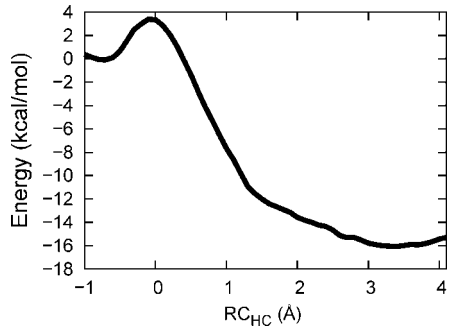

Figure 9. Energy profile of the protonation of Cys185 by His187.

way on its interaction with His187. This residue stabilizes the thiolate by charge−charge interaction and by hydrogen bonding to it with both the imidazole side chain and the NH backbone. These interactions acidify Cys185 facilitating its proton donor role.

3.4. Reprotonation by His187. During the enantiomeric inversion the nascent negative net charge that appears in Cys185 attracts His187 (which is protonated) up to a distance of 2.90 Å between the Sγ atom of Cys185 and the Nδ atom of His187. From this distance the reprotonation of Cys185 by His187 can easily take place as shown in Figure 9, where the corresponding potential energy profile on the QM(AM1)/MM PES as a function of the reaction coordinate RC_{HC} is shown. The potential energy barrier height of the reaction is only ∼4 kcal/mol, and the product is stabilized by 16 kcal/mol. Thus, this reprotonation is thermodinamically favored, as Cys185 is a less acidic residue than His187. The kinetics and thermodynamics of this step are favored by the migration along the proton transfer of the ammonium group of the substrate from Cys185 to His187. The distance between one of the protons Hτ of the D-glutamate ammonium group and the nitrogen from the histidine that donates the proton to Cys185 decreases from 4.1 to 2.7 Å, greatly stabilizing the product corresponding to this step.

The acid/base behavior of Cys185, as explained before, highly depends on its interaction with His187. pK_a calculations from selected snapshots along the Molecular Dynamics simulations clearly show this dependence. When the His187−Cys185 interaction is lost (Cys185-*S*γ−His187-*N*δ distance of 5.87 Å), the pK_a value of Cys185 is 12.11. In contrast, a structure with the His187 at a distance of 3.59 Å decreases the Cys185 pK_a up to 5.44 units. According to the PROPKA calculations, Tyr188 could as well perturb the pK_a of Cys185 (Δ pK_a of 1.37 units), but we think that the major role of this residue is more structural than catalytic, as this is not a conserved residue and the sequence alignment shows that it can be substituted by a phenylalanine, another residue with an aromatic ring. Likewise, the next residue is a strictly conserved Pro189 that marks a change in the secondary structure of the enzyme, ending the loop where this part of the active site belongs. Thus, it also seems to play a structural role. His187 also undergoes a strong desolvation effect. As it is a residue supporting a positive net charge, this fact provokes an acidifying effect (ΔpK_a of −2.54). Thus, the enzyme pocket enhances the proton donor role of this residue. Apart from this, as mentioned above, the pK_a of His187 depends on the salt-bridge interaction that it forms with an strictly conserved residue, Glu153. This glutamate only interacts with His187, and its function is to keep His187 situated close to Cys185.

4. Conclusions

In this paper we have carried out Molecular Dynamics simulations with a Molecular Mechanics force field and then a quite complete exploration of the QM/MM potential energy surfaces to study the D-glutamate to L-glutamate reaction catalyzed by BsRacE. This reaction actually occurs efficiently in spite of the fact that it requires the deprotonation of the α-carbon of the substrate, whose pK_a in aqueous solution is greater than 20, and the existence of deprotonated cysteines in the active site which are able to act as catalytic bases.

It is impossible to explore all the mechanisms one could imagine for a chemical reaction, especially for an enzyme reaction. However, using chemical intuition and all the existent previous information, one can select the most reasonable possibilities and explore them. In this case, the Molecular Dynamics simulations we have presented here show that the arrangement and the capacity of motion of the different residues around the substrate in the active site suggest no other than the mechanism we have calculated in sections 3.2−3.4. In addition this mechanism agrees with the mechanism proposed by Glavas and Tanner[6,8,19] who have suggested that the two cysteines in the active site are neutral thiols most of the time and that an aspartate and a histidine assist the catalytic thiols in acting as bases. Our results have shown that this mechanism is plausible, and we provide here a detailed molecular view of it. The whole process involves four successive proton transfers that occur in three different steps. In the enzyme/D-glutamate Michaelis complex both cysteines (Cys74 and Cys185) are not deprotonated, but neutral, as it corresponds to the normal pK_a of a cysteine. All the residues undergo important fluctuations of their position with time, but the interactions and distances evolve in such a way that the Michaelis complex is already prepared to make the first proton transfer (from Cys74 to Asp10) possible. This way, a deprotonated Cys74, which has to act as a catalytic base, is generated. In addition, the arrangement and the mobility of the different residues around the substrate are adequate to assist the subsequent three proton transfers.

Once Cys74 is deprotonated the enantiomeric inversion of the α-carbon of the substrate happens. This second step involves two proton transfers (from the α-carbon to Cys74, and from Cys185 to the α-carbon), which occur in a concerted manner, although highly asynchronic: the deprotonation of the α-carbon clearly precedes the reprotonation. Finally, in the third step, the nascent deprotonated Cys185 is protonated by His187. In other words, Cys185 does not remain as a stable deprotonated species either.

The global process consists of the interconversion of D-glutamate to L-glutamate and the transfer of a proton from His187 to Asp10, the two cysteines in the active site beginning and finishing as neutral species. The whole reaction turns out to be an exoergic process, as a consequence of three successive exoergic steps. An important point has to be clarified here. Starting form the free Enzyme (E) in solution and the free D-glutamate (S_D) in solution, the actual, complete racemization reaction takes place in a number of successive steps:

$$E + S_D \xrightarrow{(1)} (ES_D) \xrightarrow{(2)} (ES_D)' \xrightarrow{(3)} (ES_L)' \xrightarrow{(4)}$$

$$(ES_L) \xrightarrow{(5)} E' + S_L \xrightarrow{(6)} E + S_L$$

Step (1) is the association reaction of free enzyme and D-glutamate to form the first Michaelis complex. Step (2) is

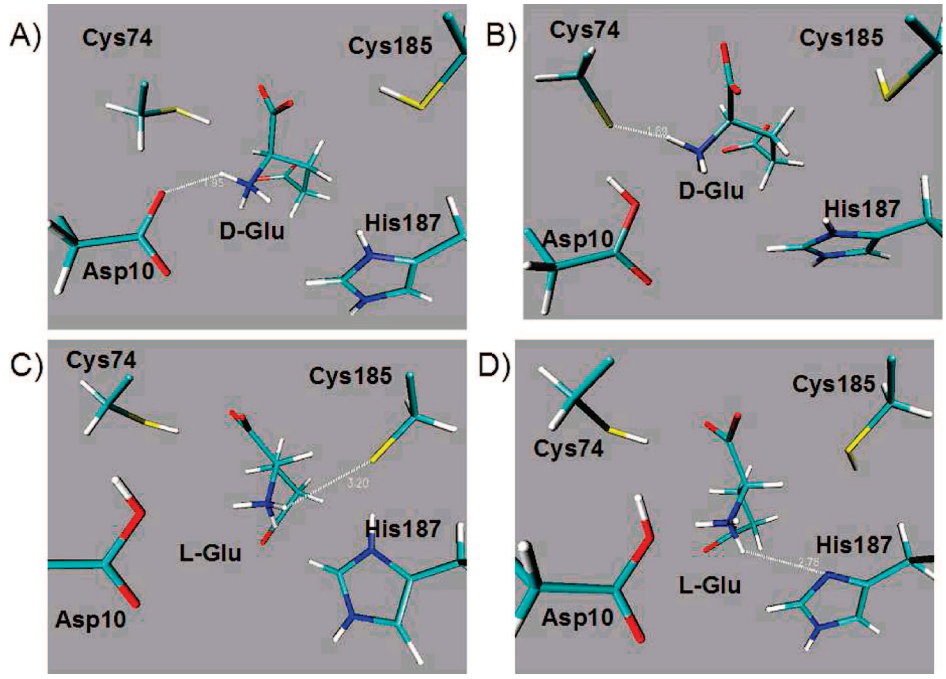

Figure 10. Complete migration of the ammonium group. (A) Interacting with Asp10 at the begining of the global reaction. (B) Interacting with Cys74 at the begining of the enantiomeric inversion. (C) Interacting with Cys185 after the enantiomeric inversion. (D) Interacting with His187 at the end of the global reaction.

the first proton transfer: from Cys74 to Asp10 (described in Figure 4A). Step (3) is the enantiomeric inversion itself (described in Figures 5 and 6), leading to a complex where the substrate is already L-glutamate (S_L). Step 4 is the reprotonation of Cys185 by His187 (described in Figure 9). Step 5 should be the release of L-glutamate. In this step the free enzyme obtained (E') is quite different from the initial E. E' is the result of the evolution of the enzyme (while forming the complex with the substrate) along the reaction, trying to favor the transformation from D-glutamate to L-glutamate. As a consequence, the differences between E and E' are important and involve changes in the protonation states of several residues and conformational changes. Finally, step (6) regenerates the initial free enzyme (E). Since S_D and S_L substrates are enantiomers, the process in all (that is, including all the 6 steps) has to be thermoneutral. However, in the present paper we have just studied steps 2−4, and our results are that (2) + (3) + (4) (note that (ES_D) and (ES_L) are not enantiomers at all) leads to an exoergic process (that is, in terms of potential energy). This result is compatible with the fact that the experimental results show that the k_{cat} (related to steps 2−4) corresponding to both isomeric directions are clearly different ($k_{cat,D} \neq k_{cat,L}$) in many of the glutamate racemases,[29] including the one from *Bacillus subtilis*.[46]

One of the most important reasons for which steps 2−4 are exergonic is the key role of the positively charged ammonium group of the substrate along the reaction, which introduces very important electrostatic interactions. This ammonium group initially interacts through a salt-bridge interaction with the ionized Asp10, efficiently contributing to its stabilization. Afterward, this ammonium group accompanies each proton transfer in a concerted and coupled way, but moving itself in the opposite direction. So, the nascent negative net charge that is created on the corresponding proton donor atom (except in the third step, where the proton donor becomes neutral) is stabilized by the interaction with the ammonium group, the corresponding proton transfer being strongly facilitated. This way, this ammonium group makes a complete migration from Asp10 to His187 (see several snapshots of this movement in Figure 10). In some sense, it can be said that the catalytic action of BsRacE glutamate racemase is driven by its own substrate in the reaction, D-glutamate. This could be a new and interesting example of the extreme complementarity and synergy between the enzyme and the corresponding substrate, which likely occurs in many other enzyme reactions.

At this point one could wonder why a proton of the positively charged ammonium group of D-glutamate is not transferred to Asp10 before the first proton transfer from Cys74 to Asp10 or to Cys74 before the enantiomeric inversion. Any of these two proton transfers from the NH_3^+ group would stop the reaction mechanism of the enzyme. However it has to be realized that the NH_3^+ group of glutamic acid is not as acidic as it would seem at first glance. In aqueous solution its pK_a is 9.5, whereas the values of the aspartic acid and cysteine side chains are 2.0 and 8.4, respectively. On the other hand, inside RacE the NH_3^+ group forms additional hydrogen bonds with Thr186 and Ser11 both when it is close to the carboxylate group of Asp10 or to the sulfur atom of Cys74. Any proton transfer from the NH_3^+ group would eliminate the positive charge of the group, so weakening the other two hydrogen bonds. For all those reasons, proton transfer from the NH_3^+ group to either Asp10 or Cys74 is not favorable.

Thus, we have arrived at a consistent proposal (very well supported by the work of others and our prior one) about a mechanism for this target biochemical process, discussing the role of the most relevant residues. However it is clear that an extensive sampling of the configurational space is required for meaningful determination of the energetics and rate of enzymatic

(46) Ashiuchi, M.; Tani, K.; Soda, K.; Misono, H. *J. Biochem.* **1998**, *123*, 1156.

reactions.[47] So, once the potential energy surface has been characterized, the next step is the introduction of the temperature effect and the free energy calculations, which are now being carried out in our laboratory.

Acknowledgment. We are grateful for financial support from the Spanish "Ministerio de Educacion y Ciencia" and the "Fondo Europeo de Desarrollo Regional" through Project CTQ2005-07115/BQU and "Generalitat de Catalunya" (2005SGR00400). M.G.-V. thanks the "Ramon y Cajal" program for financial support. E.M. receives financial support from CONACyT (Fellowship No. 302244). We want to acknowledge Dan Thomas Major and Jiali Gao for sharing the AM1-SRP parameters they developed for the alanine racemase reaction and for helpful discussions.

Supporting Information Available: Complete ref 37, computed gas phase proton affinities, interaction energies with water, and optimized van der Waals parameters. This material is available free of charge via the Internet at http://pubs.acs.org.

JA806012H

(47) Klahn, M.; Braun-Sand, S.; Rosta, E.; Warshel, A. *J. Phys. Chem. B* **2005**, *109*, 15645.